Downregulation of ACC expression suppresses cell viability and migration in the malignant progression of breast cancer

MEI JIN[1], CHUNLEI YUAN[2], SIJIA DUAN[2], BIN ZENG[3] and LINGJUAN PAN[4]

[1]Department of Galactophore, The Second Affiliated Hospital of Nanchang University, Nanchang, Jiangxi 330006; [2]Department of Galactophore Surgery, The Second Affiliated Hospital of Nanchang University, Nanchang, Jiangxi 330006; [3]Department of General Surgery, Nanchang University, Nanchang, Jiangxi, 330031; [4]Department of General Surgery, Fengcheng People's Hospital, Fengcheng, Jiangxi 331100, P.R. China

Received September 5, 2022; Accepted March 16, 2023

DOI: 10.3892/etm.2023.12144

Abstract. Exploring new diagnostic biomarkers and molecular targets is of great importance in breast cancer treatment. The present study investigated the effects of acetyl-CoA carboxylase (ACC) expression interference on the malignant progression of breast cancer cells. ACC expression was knocked down using a lentiviral vector and this was verified by quantitative polymerase chain reaction and western blotting. MCF-7 and MDA-MB-231 breast cancer cells were randomly allocated into the following groups: Normal breast cancer cells (control), breast cancer cells transduced with a negative control lentiviral vector and breast cancer cells transduced with an ACC knockdown lentiviral vector. Screening for stable transgenic strains was successful. Cell viability, apoptosis and migration were determined using Cell Counting Kit-8, flow cytometry and scratch test, respectively. The protein expression levels of N-cadherin, Vimentin and Bax were detected by western blotting. In addition, a nude mouse model of subcutaneous metastatic tumor was established using MCF-7 breast cancer cells, and tumor volume was assessed. Furthermore, pathological condition and apoptosis were detected using hematoxylin and eosin, and TUNEL staining, respectively. The protein expression levels of N-cadherin, Vimentin and Bax were detected by western blotting. The *in vitro* experiments showed that knockdown of ACC expression significantly decreased the viability and migration, and increased the apoptosis of MCF-7 and MDA-MB-231 breast cancer cells. *In vivo* experiments revealed that ACC knockdown effectively reduced the tumor volume in nude mice, and promoted tumor cell apoptosis. Both *in vitro* and *in vivo* experiments showed that ACC knockdown can reduce the protein expression levels of N-cadherin and Vimentin, and increase Bax expression. These findings suggested that downregulation of ACC expression may significantly reduce the malignant progression of breast cancer, and could be considered a potential therapeutic target.

Correspondence to: Dr Lingjuan Pan, Department of General Surgery, Fengcheng People's Hospital, 533 Ziyunnan Avenue, Xincheng, Fengcheng, Jiangxi 331100, P.R. China
E-mail: lingjuanpan@163.com

Key words: breast cancer, ACC gene, proliferation, migration, apoptosis

Introduction

Breast cancer is the most common malignant tumor in women worldwide and is also the main cause of cancer-associated mortality in women (1). The most common treatments for breast cancer include surgery, chemotherapy, hormone therapy and radiotherapy; however, breast cancer is highly heterogeneous and these therapies are often ineffective for the treatment of breast cancer metastasis (2). Breast cancer cell proliferation, metastasis and malignant progression are the main causes of cancer-related death (3). Therefore, exploring new diagnostic biomarkers and molecular targets is of great importance in the treatment of breast cancer.

Acetyl-CoA carboxylase (ACC) is a biotin-dependent enzyme, which can be used as a catalyst for CO_2 carboxylation and conversion of acetyl-CoA to malonyl-CoA (4). ACC is highly enriched in adipogenic tissues, and is under long term control at the transcriptional and translational levels through targeted phosphorylation/dephosphorylation of serine residues and sterol conversion of citrate or palmitoyl-CoA (5). In recent years, numerous studies have focused on the role of ACC in cancer. Zhan *et al* (6) identified ACC as an antitumor target in colon cancer. Zhao *et al* (7) reported that the expression levels of ACC in ovarian cancer stem cells were significantly increased. In addition, ACC has been reported to be overexpressed in liver cancer, where it can promote the proliferation of human hepatoma HepG2 cells and the rat liver cell line BRL3A (8). ACC has been shown to be overexpressed in gastric cancer, and ACC/phosphorylated-ACC has been considered a potential target for cancer treatment (9). However, the role of ACC in breast cancer remains unclear.

The present study aimed to determine the role of ACC in the malignant progression of breast cancer proliferation and metastasis. Lentiviral-mediated short hairpin RNA (shRNA) was used to knock down the expression of ACC in two breast cancer cell lines (MCF-7 and MDA-MB-231), and its functions were subsequently explored. In addition, a nude mouse model of

subcutaneous metastatic tumors was established, and the results were compared with the findings from breast cancer cells. It was hypothesized that the ACC gene may affect cell viability and migration in the malignant progression of breast cancer.

Materials and methods

Experimental animals and cells. A total of 12 female 4-week-old nude mice [Changzhou Cavens Laboratory Animal Co., Ltd.; license no. SCXK (Su) 2016-0010], weighing ~20 g, were raised under the following conditions: Temperature, 20-26˚C; humidity, 40-70%; with *ad libitum* access to specific-pathogen-free grade animal feed and sterilized drinking. Human MCF-7 (TCHu 74) and MDA-MB-231 (TCHu227) triple-negative breast cancer cells were obtained from The Cell Bank of Type Culture Collection of The Chinese Academy of Sciences. The cells were cultured in high-glucose Dulbecco's modified Eagle's medium (DMEM; cat. no. KGM12800S; Nanjing KeyGen Biotech Co., Ltd.), containing 10% fetal bovine serum (FBS; cat no. 10099-141; Gibco; Thermo Fisher Scientific, Inc.) and 1% penicillin-streptomycin (cat. no. P1400; Beijing Solarbio Science & Technology Co., Ltd.) at 37˚C in a humidified atmosphere containing 5% CO_2. The interim cell line 293T and the pLKO.1-EGFP Puro plasmid were purchased from Hanbio Biotechnology Co., Ltd.

Main reagents and instruments. Polyethylene glycol (PEG)8000 (cat no. 81268) was from MilliporeSigma. The Annexin V-FITC/PI Apoptosis Kit (cat. no. AP101-100-kit) was purchased from MultiSciences (Lianke) Biotech, Co., Ltd. Ultrapure RNA Kit (cat. no. CW0581M) was purchased from CoWin Biosciences. HiScript II Q RT SuperMix for quantitative polymerase chain reaction (qPCR) (+gDNA wiper) (cat. no. R223-01) was from Vazyme Biotech Co., Ltd. 2X SYBR Green PCR Master Mix (cat. no. A4004M) was purchased from Xiamen LifeInt Technology Co., Ltd. Radioimmunoprecipitation assay buffer (cat. no. C1053) was obtained from Applygen Technologies Inc. Polyvinylidene difluoride membranes (cat. no. IPVH00010) were purchased from MilliporeSigma. Mouse monoclonal anti-GAPDH internal loading control antibody (1:2,000; cat. no. TA-08), and goat anti-mouse IgG (H+L) HRP conjugate (1:2,000; cat. no. ZB-2305) and goat anti-rabbit IgG (H+L) HRP conjugate (1:2,000; cat. no. ZB-2301) secondary antibodies were obtained from OriGene Technologies, Inc. The following primary antibodies were used in the present study: Rabbit anti N-cadherin (1:1,000; AF4039; Affinity Biosciences, Ltd.), rabbit anti-vimentin (1:2,000; cat. no. 10366-1-ap), rabbit anti-Bax (1:5,000; cat. no. 50599-2-lg) (both from Proteintech Group, Inc.). Scott's Bluing Solution (cat. no. G1865) was obtained from Beijing Solarbio Science & Technology Co., Ltd. The TUNEL assay kit (cat. no. C1090) was purchased from Beyotime Institute of Biotechnology. Minimum Essential Medium (MEM) high glucose complete medium (cat no. KGM41500S) and Cell Counting Kit-8 (CCK-8) cell proliferation detection kit (cat. no. KGA317) were obtained from Nanjing KeyGen Biotech Co., Ltd. The NovoCyte™ flow cytometer (NovoCyte 2060R) was from ACEA Bioscience, Inc. The fluorescence PCR machine (CFX Connect™ Real-Time) and the ultra-sensitive chemiluminescence imaging system (Chemi Doc™ XRS+) were from Bio-Rad Laboratories, Inc. The automated microplate reader (WD-2102B) and vertical protein electrophoresis system (DYY-6C) were purchased from Beijing Liuyi Instrument Factory. An inverted fluorescence microscope (MF53) was from Guangzhou Micro-shot Technology Co., Ltd., and a CX41 fluorescence microscope was obtained from Olympus Corp.

Table I. shRNA sequences.

shRNA	Sequence, 5'-3'
ACC shRNA-1	TACAAGGGATACAGGTATTTA
ACC shRNA-2	TATGAGGTGGATCGGAGATTT
ACC shRNA-3	GTATGTTCGAAGGGCTTATAT
NC	TAGGCTAGGCGTAGCTATAGC

ACC, acetyl-CoA carboxylase; shRNA, short hairpin RNA; NC, negative control.

Selection of shRNA. According to the sequence of ACC, three shRNAs were selected on a shRNA design website (https://www.sigmaaldrich.cn/CN/zh/semi-configurators/shrna?activeLink=selectClones) and cloned into the pLKO.1-EGFP Puro plasmid. The 3rd generation system was used for lentiviral transduction and the interim cell line was 293T. Four plasmids (12 μg lentiviral plasmid + 12 μg Lenti-Mix=24 μg total; Lenti-Mix was composed of pMDLg/pRRE : pVSV-G : pRSV-Rev, 5:3:2) was added into a 5 ml Eppendorf (EP) tube for transfection of 293T cells to produce lentiviral vectors. Subsequently, 1,000 μl 0.25 M $CaCl_2$ was added, and gently mixed evenly with a pipette. Then, 1,000 μl 2X HBS was added, gently mixed evenly with the pipette, and let stand at room temperature for 10 min. Finally, the Lenti-DNA Mix transfection system solution was added dropwise to the culture dish of the 293T cells, the dish was gently agitated to mix well, and cultured in a 37˚C cell culture incubator containing 5% CO_2.

A total of 8-10 h after transfection, the culture medium was replaced with 20 ml prewarmed complete medium and culture was continued. A total of 24 h after transfection, observation was performed under a fluorescence microscope and images were captured. Subsequently, 72 h after transfection, the cell culture supernatant was collected, and centrifuged at 3,000 x g and 4˚C for 10 min. Then, the supernatant was obtained, filtered through a 0.45-μM filter and fully mixed with 5X PEG8000 lentivirus concentration solution overnight at 4˚C. On the second day, centrifugation was performed at 10,000 x g at 4˚C for 30 min, and the lentiviral particles were resuspended in 1 ml serum-free DMEM, aliquoted and stored at -80˚C.

The interference efficiencies of the shRNAs were detected by qPCR. The shRNA with the best effect was selected for further experiments. The sequences of the three ACC shRNAs are listed in Table I.

Cell transduction, stable screening and grouping. MCF-7 and MDA-MB-231 cells were transduced with the indicated lentiviruses. The cell culture medium was replaced with

Table II. Primer information.

Primer name	Primer sequence, 5'-3'	Primer length, nt	Product length, bp	Annealing temperature, ˚C
ACC	F: GGACCCAGTCTACATCCACT	20	194	57.65
	R: TATCGCTAATAACACCCTTCTCC	23		
GAPDH	F: TGACTTCAACAGCGACACCCA	21	121	61.5
	R: CACCCTGTTGCTGTAGCCAAA	21		

ACC, acetyl-CoA carboxylase; F, forward; R, reverse.

serum-free medium (1 ml). The multiplicity of infection (MOI) was $3x10^8$ TU/ml and the duration of transduction into cells was 8-10 h. The time interval between transduction and subsequent experimentation was 48 h. Puromycin (2.5 μg/ml) was added to the stably expressed cells post-transduction and the medium was changed every 2 days. If, under the CX41 fluorescence microscope, the proportion of fluorescent cells was 100%, and they could be subcultured and expanded normally, this indicated that the screening of the stable transgenic strains was successful.

The cells were randomly allocated into the following groups: i) Normal breast cancer cells (control group), ii) breast cancer cells transduced with a negative control (NC) lentiviral plasmid, and iii) breast cancer cells transduced with a shRNA ACC lentiviral plasmid (shACC).

Reverse transcription (RT)-qPCR. TRIzon from the Ultrapure RNA Kit was used to completely lyse the sample and extract RNA from the tumor tissue ; RNA concentration and purity were then determined. cDNA was synthesized from RNA using HiScript II Q RT SuperMix, according to the manufacturer's protocol. Using cDNA as the template, qPCR was performed using a fluorescence qPCR instrument; with GAPDH used as the internal reference gene, the relative mRNA expression levels of the genes of interest in each group were calculated. The reaction system was as follows: 2X SYBR Green PCR Master Mix (10 μl), cDNA (1 μl), upstream primer (0.4 μl), downstream primer (0.4 μl), RNase-free ddH_2O (8.2 μl). The reaction steps were as follows: Pre-denaturation at 95˚C for 10 min; followed by 40 cycles of denaturation at 95˚C at 10 sec, annealing at 58˚C for 30 sec and extension at 72˚C for 30 sec. The primer sequences are shown in Table II. GAPDH was used as the internal reference, and the relative expression levels of ACC were calculated according to the $2^{-\Delta\Delta Cq}$ method (10).

Western blotting. The cell culture medium was removed from the culture dish using a pipette. Subsequently, 100 μl cell lysis buffer was added to each well and placed on ice for 20 min. The cells were scraped to one side with a cell scraper and then transferred to EP tubes, which were centrifuged at 13,523 x g at 4˚C for 10 min, and the supernatant was used to assess total protein concentration using a bicinchoninic acid kit. The proteins were then denatured, loaded (50 μg/lane), separated by SDS-PAGE on 12% gels for 2 h, and transferred to membranes at a constant current of 300 mA for 80 min. The membranes were incubated with 5% skimmed milk at room temperature for 1.5 h. After blocking, they were incubated with the primary antibodies at 4˚C overnight, and with the secondary antibody at room temperature for 2 h. Drops of ECL luminescent liquid were added to the membranes and exposed in the gel imaging system. ImageJ software (version 1.8.0, National Institutes of Health) was used to analyze the gray value of each band.

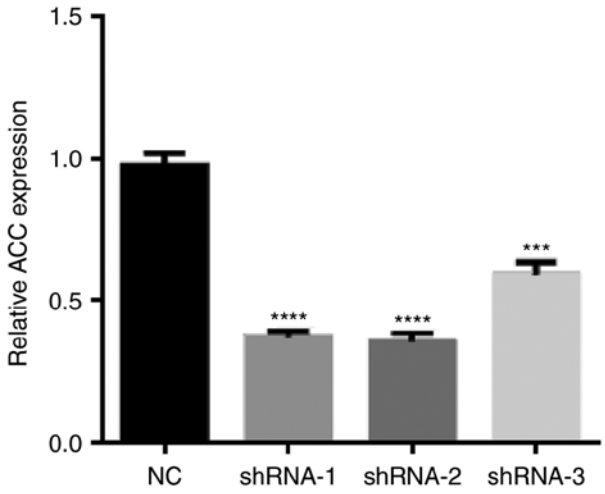

Figure 1. Selection of ACC shRNA. ***P<0.001, ****P<0.0001 vs. NC group. ACC, acetyl-CoA carboxylase; NC, negative control; shRNA, short hairpin RNA.

CCK-8 cell viability assay. The groups of cells were digested, resuspended, counted and plated at a cell density of $5x10^3$ cells/well in a 96-well plate. The cells were then cultured for 48 h in MEM. Subsequently, the culture medium was discarded and replaced with the same medium (100 μl per well). CCK-8 reagent was added to each well and placed in the incubator at 37˚C for 2 h. The absorbance of each well was detected at a wavelength of 450 nm using a microplate reader and the cell viability rate was calculated using the following formula: Cell viability rate (%)=(experimental group cell OD/control group OD) x100.

Apoptosis detected by flow cytometry. Cells ($1-3x10^6$) were collected, added to 1 ml PBS, centrifuged at 300 x g at 4˚C for 3 min, and washed twice. Binding buffer (5X) was diluted into 1X binding buffer with double distilled water and 300 μl pre-cooled 1X binding buffer was used to resuspend the cells. Subsequently, 5 μl Annexin V-FITC and 10 μl

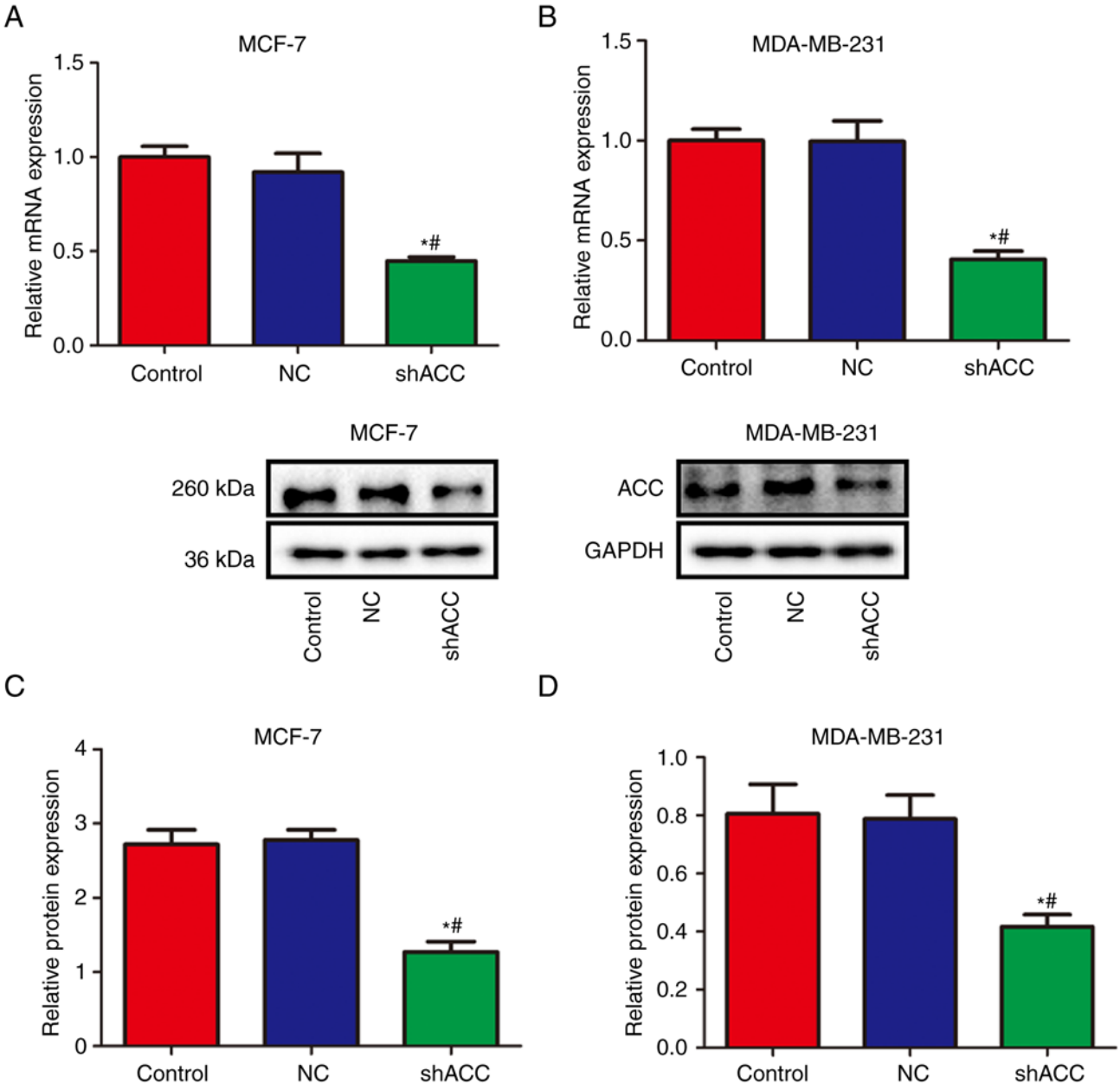

Figure 2. Effects of ACC gene interference. mRNA expression levels of ACC were detected in (A) MCF-7 and (B) MDA-MB-231 cells by reverse transcription-quantitative PCR. Protein expression levels of ACC were detected in (C) MCF-7 and (D) MDA-MB-231 cells by western blotting. *P<0.05 vs. Control group; #P<0.05 vs. NC group. ACC, acetyl-CoA carboxylase; NC, negative control; sh, short hairpin.

PI were added to each tube, mixed slightly and incubated at room temperature for 10 min in the dark. Finally, 200 μl pre-cooled 1X binding buffer was added to each tube, mixed and apoptosis was detected by the NovoCyte flow cytometer using the NovoExpress software (version 1.5.6; Agilent Technologies, Inc.)

Cell migration detected by cell scratch test. Once the cell density reached ≥90%, the scratch test was performed. A 200-μl pipette tip was used to scratch each well, the medium was discarded, the cells were washed three times with PBS and the medium was replaced with serum-free medium. Images of the wound were captured with an inverted fluorescence microscope (MF53) at 0 h and after 24 h in an incubator at 37˚C. The scratch width was measured at 0 and 24 h, and the cell migration rate was calculated, as follows: Migration rate=migration distance/migration time.

Establishment of a nude mouse tumor model and grouping. Mice were randomly allocated into the following experimental groups: i) Normal breast cancer cells (Control), ii) breast cancer cells transduced with a NC lentiviral plasmid, and iii) breast cancer cells transduced with shACC (n=4/group).

A nude mouse model of subcutaneous metastatic tumor was established using MCF-7 breast cancer cells. Four nude mice in each group were inoculated with MCF-7 breast cancer cells ($1x10^7$ cells/mouse; 0.20 ml/mouse) subcutaneously into the armpit. For mice in the NC and shACC groups, the breast cancer cells were transduced with NC lentiviral plasmid or shACC, respectively.

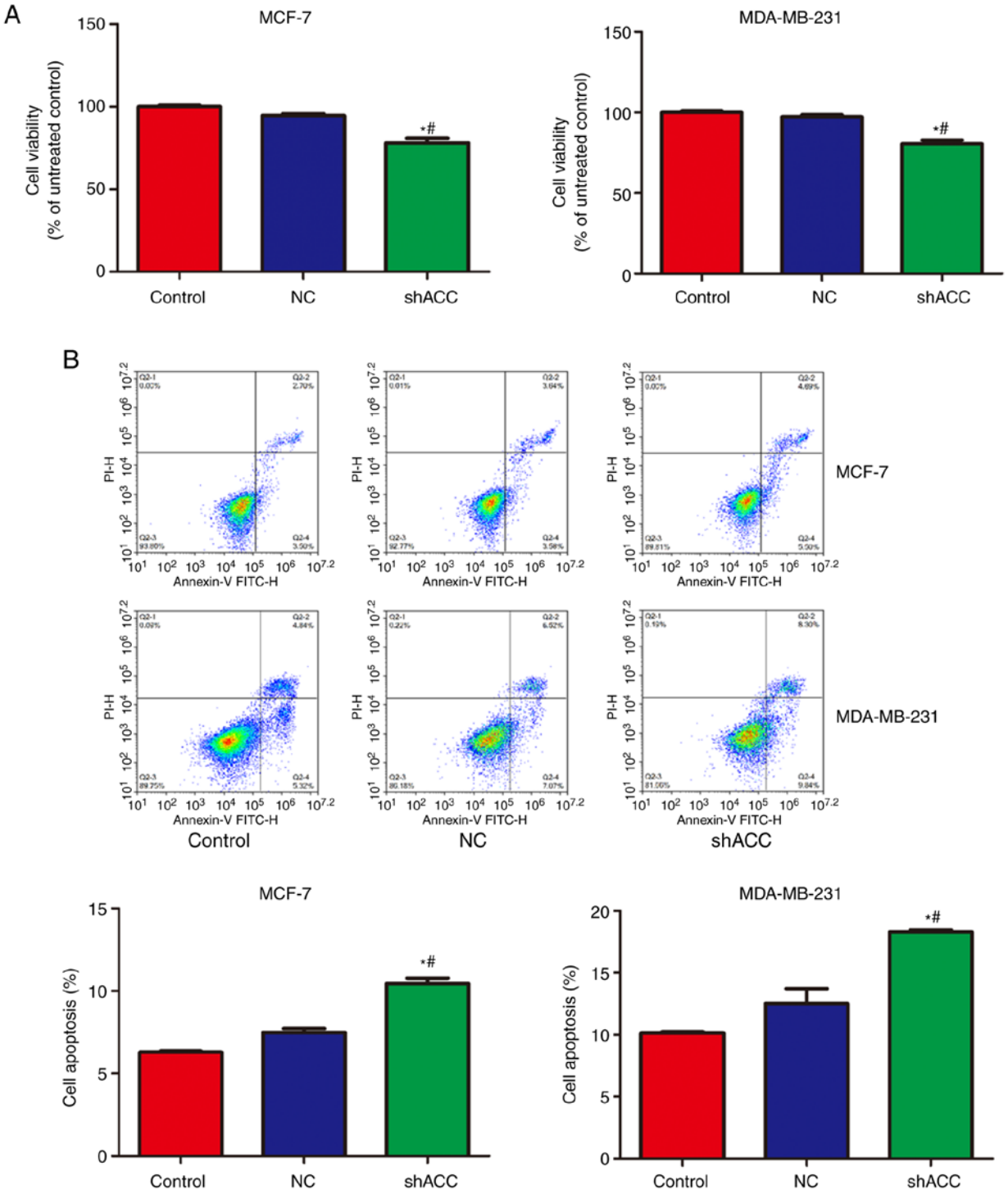

Figure 3. Effects of ACC gene interference on cell viability and apoptosis. (A) Cell viability and (B) apoptosis. *P<0.05 vs. Control group; #P<0.05 vs. NC group. ACC, acetyl-CoA carboxylase; NC, negative control; sh, short hairpin.

A total of 21 days after inoculation, the mice were euthanized by CO_2 inhalation (flow rate, 40% of the chamber volume/min) and the tumor tissue was collected. The tumor length and width were measured every 3 days after inoculation, and the tumor volume was calculated according to the following formula: Tumor volume=0.5 x long diameter x short diameter^2.

Hematoxylin and eosin (H&E) staining. The tissues were collected, fixed in 4% paraformaldehyde at 4˚C for >24 h, dehydrated, paraffin embedded and sliced into 4 μm sections, which were dewaxed and hydrated. The sections were placed in distilled water, and were then stained in hematoxylin aqueous solution for 3 min, differentiated with hydrochloric acid ethanol differentiation solution for 15 sec, slightly washed, bluing the hematoxylin stain with Scott's Bluing Solution for 15 sec, and washed with running water. Subsequently, the sections were stained with eosin for 3 min, washed with running water, dehydrated, cleared, mounted and examined under a microscope (CX43).

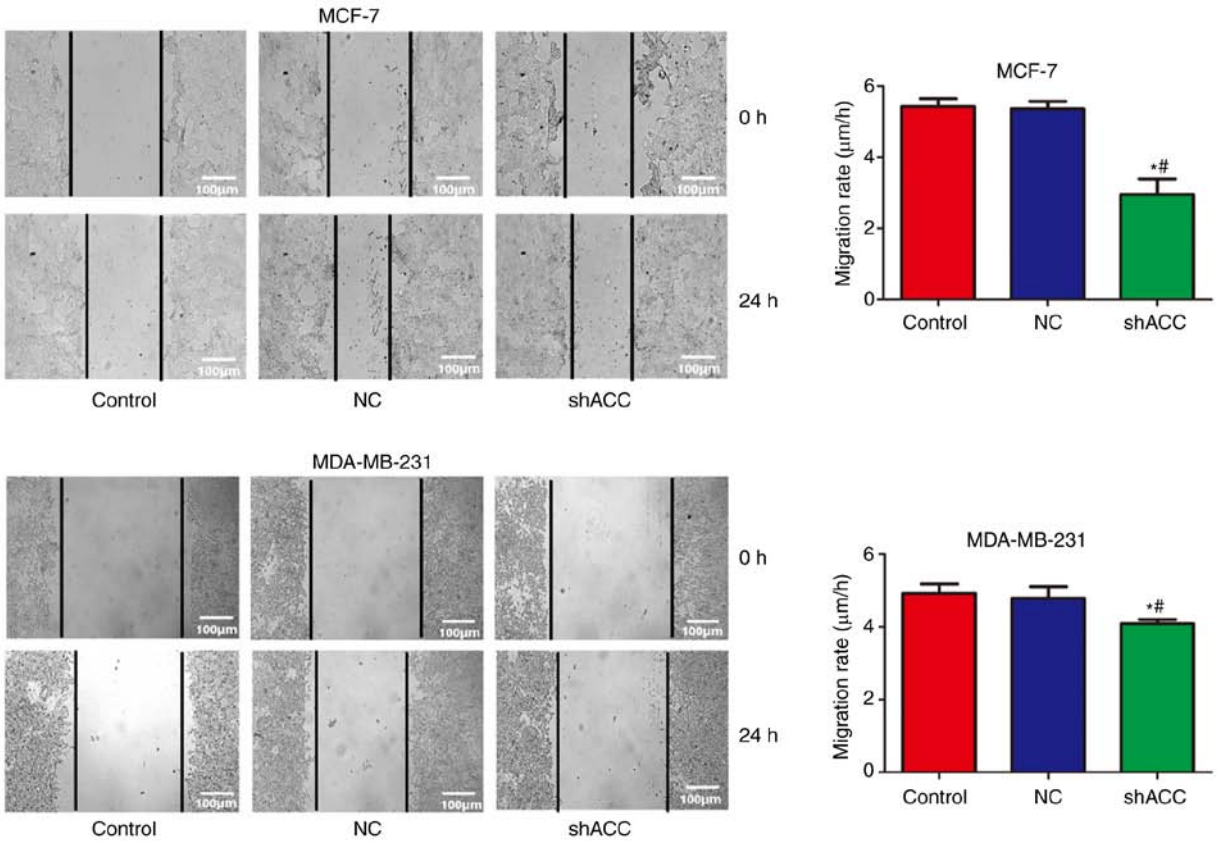

Figure 4. Effects of ACC gene interference on cell migration, as determined by cell scratch test. *P<0.05 vs. Control group; #P<0.05 vs. NC group. ACC, acetyl-CoA carboxylase; NC, negative control; sh, short hairpin.

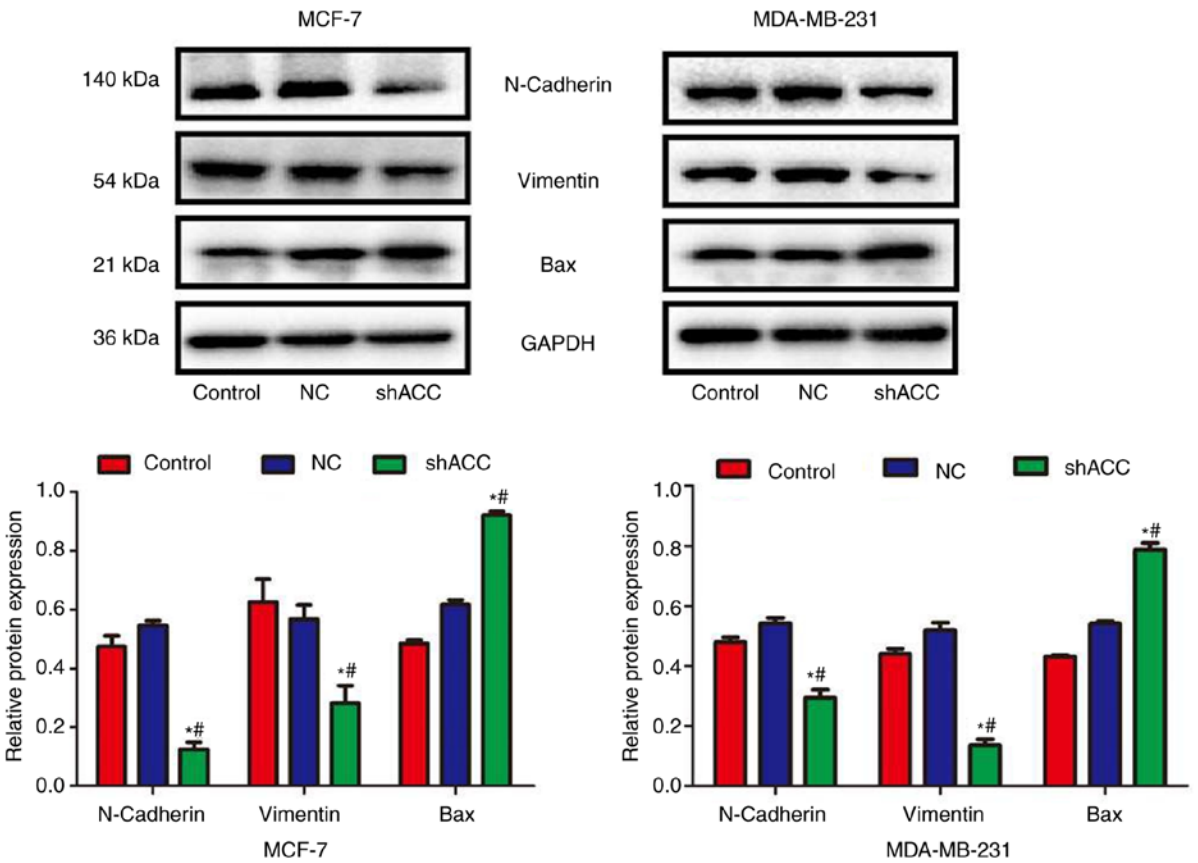

Figure 5. Effects of ACC gene interference on relative protein expression detected by western blotting. *P<0.05 vs. Control group; #P<0.05 vs. NC group. ACC, acetyl-CoA carboxylase; NC, negative control; sh, short hairpin.

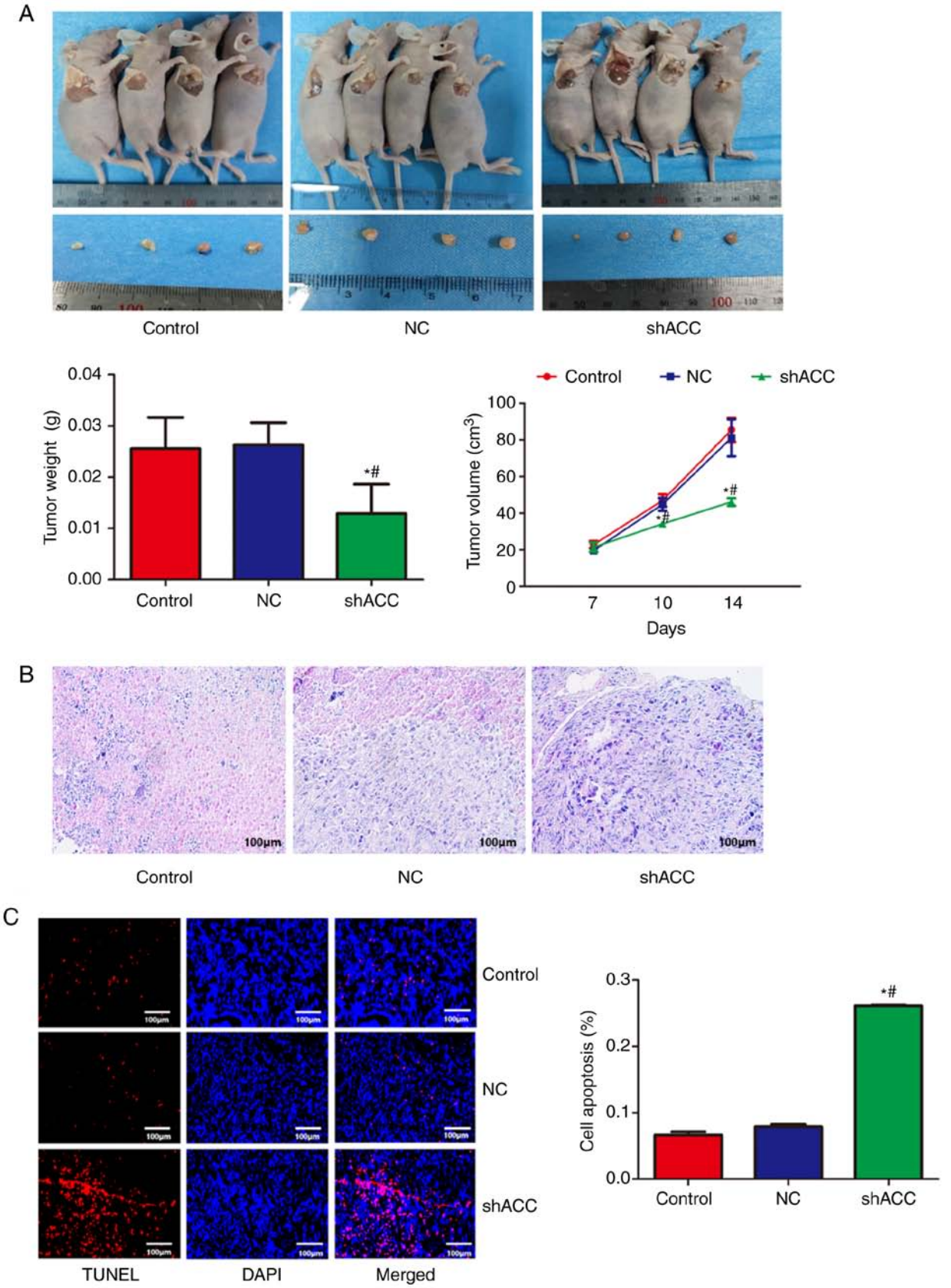

Figure 6. Effect of ACC gene interference on a MCF-7 nude mice xenograft model. (A) Tumor size, (B) hematoxylin and eosin staining, and (C) TUNEL detection of apoptosis. *P<0.05 vs. Control group; #P<0.05 vs. NC group. ACC, acetyl-CoA carboxylase; NC, negative control; sh, short hairpin.

Apoptosis detected by TUNEL staining. The tissues were fixed in 4% paraformaldehyde at 4˚C for >24 h, dehydrated, paraffin-embedded and sectioned. The paraffin-embedded sections (0.3 μm) were baked, dewaxed and hydrated. The sections then underwent antigen retrieval by the dropwise addition of Proteinase K working solution at 37˚C for 25 min,

and were washed. A sufficient amount of TUNEL test solution was added to each slide (2 μl TdT enzyme and 48 μl fluorescence labeling solution for one sample) and incubated in the dark at 42˚C for 1 h. The nucleus was counterstained by adding DAPI dropwise and incubating for 3 min in the dark at room temperature, after which, the slides were mounted with antifade mounting medium and observed under a fluorescence microscope.

Statistical analysis. SPSS 19.0 software (IBM Corp.) was used for statistical analysis. All experiments were repeated three times and the quantitative results are expressed as the mean ± standard deviation. One way ANOVA was used to compare the results among multiple groups, and the least significant difference method was used for pairwise comparison. $P<0.05$ was considered to indicate a statistically significant difference. GraphPad Prism 5.0 (GraphPad Software; Dotmatics, Inc.) was used for graph generation and ImageJ software (version 1.8.0; National Institutes of Health) was used for gray value analysis.

Results

shACC selection. Compared with the NC group, shRNA-1 had the best effect on ACC expression (Fig. 1); therefore, this shRNA was selected for further experimentation.

Effects of shACC on ACC expression. Compared with those in the Control and NC groups, the mRNA and protein expression levels of ACC were significantly decreased in the shACC groups in both breast cancer cell lines (Fig. 2). These findings suggested that ACC gene interference was effective and successfully verified, and subsequent experiments could be performed.

Effects of shACC on cell viability and apoptosis. As shown in Fig. 3, compared with that in the Control and NC groups, cell viability was significantly decreased in the shACC groups of both breast cancer cell lines, whereas apoptosis was significantly increased. These findings indicated that ACC gene interference inhibited cell viability and promoted apoptosis.

Effects of shACC on cell migration. Compared with that in the Control and NC groups, the cell migration rate was significantly decreased in the shACC groups of both breast cancer cell lines (Fig. 4). These findings suggested that ACC gene interference inhibited cell migration.

Effects of shACC on protein expression. Compared with those in the Control and NC groups, the protein expression levels of N-cadherin and Vimentin were significantly decreased in the shACC groups of both breast cancer cell lines, whereas Bax protein expression was significantly increased (Fig. 5). These findings indicated that ACC gene interference could affect the epithelial-mesenchymal transition (EMT) of cells and the expression of apoptosis-related proteins.

Effects of shACC on a MCF-7 xenograft model. A nude mouse model of subcutaneous metastatic tumor was established. As shown in Fig. 6A, compared with that in the Control and NC groups, the tumor volume was significantly decreased in the shACC group, demonstrating that ACC gene interference could reduce tumor volume in nude mice. As shown in Fig. 6B, the pathological findings showed that the breast cancer cells in the Control and NC groups were flat and surrounded by antenna-like extensions. By contrast, in the shACC group, the breast cancer cells became round and smaller, decreased in number, with pyknotic nuclei and apoptotic bodies observed, and chromatin agglutinated into patches or crescent-shaped edges. As shown in Fig. 6C, compared with that in the Control and NC groups, the apoptosis rate of the breast cancer cells in the shACC group was significantly increased, suggesting that ACC gene interference promoted apoptosis.

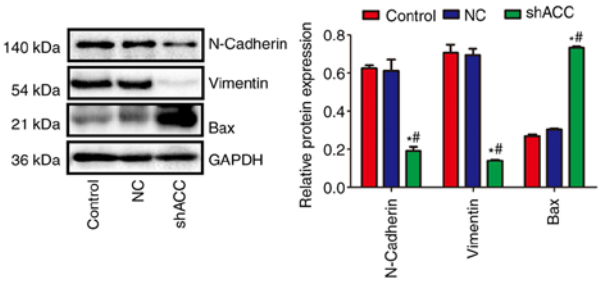

Figure 7. Effect of ACC gene interference on related protein expression detected by western blotting in tumor tissues. *P<0.05 vs. Control group; #P<0.05 vs. NC group. ACC, acetyl-CoA carboxylase; NC, negative control; sh, short hairpin.

Effects of shACC on protein expression in a MCF-7 xenograft model. Compared with those in the Control and NC groups, the protein expression levels of N-cadherin and Vimentin were significantly decreased in the shACC group, whereas the protein expression levels of Bax were significantly increased (Fig. 7). This finding confirmed that ACC gene interference also affected the EMT of cells and the expression of apoptosis-related proteins *in vivo*.

Discussion

Notable progress has been made in understanding the signaling network regulating breast cancer pathogenesis (11); however, due to various reasons, such as tumor heterogeneity, drug resistance and drug-induced toxicity (12), exploring effective therapeutic targets remains a key issue that urgently needs to be solved in breast cancer. Excessive cell proliferation and metastasis of tumor cells are typical features of malignant lesions. Compared with in normal human tissues, tumor cells prefer to use exogenous lipids to promote growth and cell viability (6). Previous studies have reported that a variety of cancer cells contain high levels of lipid-related enzymes (13), including ACC (14), which can significantly promote the malignant characteristics of high proliferation and metastasis (15).

It has been shown that ACC is a valuable drug target for the treatment of various metabolic diseases (4), including hepatic steatosis (16), nonalcoholic fatty liver disease, metabolic syndrome (17), obesity and hepatic insulin resistance (18). Previous studies have demonstrated that ACC is also a potential cancer treatment target. In prostate cancer (19) and liver cancer (8) cells, knocking down ACC can inhibit cancer proliferation and induce apoptosis without cytotoxic effects

on normal cells. The present study focused on two types of breast cancer cell lines, MCF-7 and MDA-MB-231, as these two types of cells are relatively representative cell lines of breast cancer. After knocking down ACC gene expression, the viability of breast cancer cells was decreased, whereas the apoptosis rate of cells was increased, and the cell migration was significantly inhibited. The results were consistent with those of previous studies (8,19). In addition, knockdown of ACC gene expression inhibited the formation and migration of nude mouse model tumors.

In order to understand the effect of ACC on the malignant progression of MCF-7 and MDA-MB-231 cells, a CCK-8 assay was used to detect the changes in cell viability after ACC knockdown. The results showed that ACC knockdown could inhibit cancer cell viability, and the results of flow cytometry also revealed that ACC knockdown could induce breast cancer cell apoptosis. EMT is the process of epithelial cells transitioning to a mesenchymal state (20), which is considered to be the main process of tumor metastasis (21). The molecular and cellular changes observed in EMT are characterized by upregulation of specific proteins, such as N-cadherin and vimentin, which are used as EMT markers (22). It has been reported that EMT may be related to the prognosis and clinicopathological features of patients with breast cancer (23). The overexpression of mesenchymal cell marker factors and expression of EMT-related transcription factors has been reported to promote metastasis in breast cancer cells (24). In order to further study the effect and mechanism of ACC on breast cancer cells, a cell scratch test was performed to detect the migratory ability of cells and western blotting was conducted to determine the expression levels of EMT-related markers. The results showed that ACC knockdown inhibited the migratory ability of breast cancer cells and decreased the expression levels of N-cadherin and vimentin. Therefore, ACC may inhibit the malignant progression of breast cancer, and cell migration and metastasis, by affecting EMT. In addition, the *in vivo* experiments revealed that knockdown of ACC gene expression could inhibit the EMT process in tumors from nude mice, which is consistent with the *in vitro* results. Future studies may evaluate the expression of ACC in clinical samples, as well as the association between ACC and survival of patients with breast cancer.

In subsequent studies, a colony formation assay may be performed to compare the findings with those of the CCK-8 assay. Experiments with other shRNAs, to exclude off-target effects, and comparison of ACC knockdown with ACC overexpression may also be performed.

In conclusion, the findings of the present study suggested that the ACC gene may affect cell viability and migration in the malignant progression of breast cancer through the EMT process. Targeting ACC expression could be used as a new target therapy for breast cancer.

Acknowledgements

Not applicable.

Funding

No funding was received.

Availability of data and materials

The datasets used and/or analyzed during the current study are available from the corresponding author on reasonable request.

Authors' contributions

MJ and LP designed the experiments. MJ, CY, SD and BZ performed the experiments and analyzed the data. MJ wrote the manuscript. LP revised the manuscript and supervised the experiments. MJ and LP confirm the authenticity of all the raw data. All authors read and approved the final manuscript.

Ethics approval and consent to participate

The present study was approved by the Ethics Committee of The Second Affiliated Hospital of Nanchang University (approval no. 2021080401; Nanchang, China).

Patient consent for publication

Not applicable.

Competing interests

The authors declare that they have no competing interests.

References

1. Dowsett M: Preoperative models to evaluate endocrine strategies for breast cancer. Clin Cancer Res 9: 502S-510S, 2003.
2. Youness RA, Gad AZ, Sanber K, Ahn YJ, Lee GJ, Khallaf E, Hafez HM, Motaal AA, Ahmed N and Gad MZ: Targeting hydrogen sulphide signaling in breast cancer. J Adv Res 27: 177-190, 2020.
3. Viedma-Rodríguez R, Baiza-Gutman L, Salamanca-Gómez F, Diaz-Zaragoza M, Martínez-Hernández G, Ruiz Esparza-Garrido R, Velázquez-Flores MA and Arenas-Aranda D: Mechanisms associated with resistance to tamoxifen in estrogen receptor-positive breast cancer (review). Oncol Rep 32: 3-15, 2014.
4. Chen L, Duan Y, Wei H, Ning H, Bi C, Zhao Y, Qin Y and Li Y: Acetyl-CoA carboxylase (ACC) as a therapeutic target for metabolic syndrome and recent developments in ACC1/2 inhibitors. Expert Opin Investig Drugs 28: 917-930, 2019.
5. Corbett JW: Review of recent acetyl-CoA carboxylase inhibitor patents: Mid-2007-2008. Expert Opin Ther Pat 19: 943-956, 2009.
6. Zhan Y, Ginanni N, Tota MR, Wu M, Bays NW, Richon VM, Kohl NE, Bachman ES, Strack PR and Krauss S: Control of cell growth and survival by enzymes of the fatty acid synthesis pathway in HCT-116 colon cancer cells. Clin Cancer Res 14: 5735-5742, 2008.
7. Zhao S, Cheng L, Shi Y, Li J, Yun Q and Yang H: MIEF2 reprograms lipid metabolism to drive progression of ovarian cancer through ROS/AKT/mTOR signaling pathway. Cell Death Dis 12: 18, 2021.
8. Ye B, Yin L, Wang Q and Xu C: ACC1 is overexpressed in liver cancers and contributes to the proliferation of human hepatoma Hep G2 cells and the rat liver cell line BRL 3A. Mol Med Rep 19: 3431-3440, 2019.
9. Fang W, Cui H, Yu D, Chen Y, Wang J and Yu G: Increased expression of phospho-acetyl-CoA carboxylase protein is an independent prognostic factor for human gastric cancer without lymph node metastasis. Med Oncol 31: 15, 2014.
10. Livak KJ and Schmittgen TD: Analysis of relative gene expression data using real-time quantitative PCR and the 2(-Delta Delta C(T)) method. Methods 25: 402-408, 2001.
11. Zhou J, Chen C, Zhao X, Jiang T, Jiang Y, Dai J and Chen J: Coding variants in the PCNT and CEP295 genes contribute to breast cancer risk in Chinese women. Pathol Res Pract 225: 153581, 2021.

12. Miller EA, Pinsky PF, Heckman-Stoddard BM and Minasian LM: Breast cancer risk prediction models and subsequent tumor characteristics. Breast Cancer 27: 662-669, 2020.
13. Rysman E, Brusselmans K, Scheys K, Timmermans L, Derua R, Munck S, Van Veldhoven PP, Waltregny D, Daniëls VW, Machiels J, *et al*: De novo lipogenesis protects cancer cells from free radicals and chemotherapeutics by promoting membrane lipid saturation. Cancer Res 70: 8117-8126, 2010.
14. Schreurs M, Kuipers F and van der Leij FR: Regulatory enzymes of mitochondrial beta-oxidation as targets for treatment of the metabolic syndrome. Obes Rev 11: 380-388, 2010.
15. Harwood HJ Jr: Treating the metabolic syndrome: Acetyl-CoA carboxylase inhibition. Expert Opin Ther Targets 9: 267-281, 2005.
16. Savage DB, Choi CS, Samuel VT, Liu ZX, Zhang D, Wang A, Zhang XM, Cline GW, Yu XX, Geisler JG, *et al*: Reversal of diet-induced hepatic steatosis and hepatic insulin resistance by antisense oligonucleotide inhibitors of acetyl-CoA carboxylases 1 and 2. J Clin Invest 116: 817-824, 2006.
17. Kusunoki J, Kanatani A and Moller DE: Modulation of fatty acid metabolism as a potential approach to the treatment of obesity and the metabolic syndrome. Endocrine 29: 91-100, 2006.
18. Srivastava RA, Jahagirdar R, Azhar S, Sharma S and Bisgaier CL: Peroxisome proliferator-activated receptor-alpha selective ligand reduces adiposity, improves insulin sensitivity and inhibits atherosclerosis in LDL receptor-deficient mice. Mol Cell Biochem 285: 35-50, 2006.
19. Pang B, Zhang J, Zhang X, Yuan J, Shi Y and Qiao L: Inhibition of lipogenesis and induction of apoptosis by valproic acid in prostate cancer cells via the C/EBPα/SREBP-1 pathway. Acta Biochim Biophys Sin (Shanghai) 53: 354-364, 2021.
20. Göbel A, Dell'Endice S, Jaschke N, Pählig S, Shahid A, Hofbauer LC and Rachner TD: The role of inflammation in breast and prostate cancer metastasis to bone. Int J Mol Sci 22: 5078, 2021.
21. Tong D: Unravelling the molecular mechanisms of prostate cancer evolution from genotype to phenotype. Crit Rev Oncol Hematol 163: 103370, 2021.
22. Barik GK, Sahay O, Behera A, Naik D and Kalita B: Keep your eyes peeled for long noncoding RNAs: Explaining their boundless role in cancer metastasis, drug resistance, and clinical application. Biochim Biophys Acta Rev Cancer 1876: 188612, 2021.
23. González-Martínez S, Pérez-Mies B, Pizarro D, Caniego-Casas T, Cortés J and Palacios J: Epithelial mesenchymal transition and immune response in metaplastic breast carcinoma. Int J Mol Sci 22: 7398, 2021.
24. Lu Y, Ding Y, Wei J, He S, Liu X, Pan H, Yuan B, Liu Q and Zhang J: Anticancer effects of traditional chinese medicine on epithelial-mesenchymal transition (EMT) in breast cancer: Cellular and molecular targets. Eur J Pharmacol 907: 174275, 2021.